

Alkalinization-Induced K^+ Current of the Mouse Megakaryocyte

Makoto Murakami¹, Naofumi Tokutomi^{2,*}, Yoshiko Tokutomi², Kimio Tomita¹ and Katsuhide Nishi²

Departments of ¹Internal Medicine and ²Pharmacology, Kumamoto University School of Medicine, Kumamoto 860–0811, Japan

Received October 5, 1998 Accepted December 21, 1998

ABSTRACT—We have recently found that mouse megakaryocytes responded to extracellular alkalinization to pH >8.0, generating a K^+ current under voltage-clamped conditions with the whole cell recording mode of the patch-clamp technique. The purpose of this study was to physiologically and pharmacologically characterize the alkaline-dependent K^+ conductance of the megakaryocyte membrane. The alkalinization-induced K^+ current (I_{ALK}) did not seem to be Ca^{2+} -dependent since I_{ALK} was allowed to be generated under intracellularly Ca^{2+} -buffered conditions with 10 mM EGTA, which completely prevented the generation of caffeine-induced Ca^{2+} -activated currents of mouse megakaryocytes; and no $[Ca^{2+}]_i$ elevation was evoked by the alkalinization protocol in contrast to a significant increase in $[Ca^{2+}]_i$ in response to caffeine when $[Ca^{2+}]_i$ was measured with a fura 2 ratiometry. I_{ALK} was strongly suppressed with tetraethylammonium (TEA), 4-aminopyridine (4-AP) and streptomycin (SM), but was completely resistant to quinidine (QND). The values of IC_{50} for the suppression of I_{ALK} with TEA, 4-AP and SM were 5.6, 0.47 and 1.5 mM, respectively. Voltage-gated K^+ currents (I_K) of the same megakaryocyte preparation were weakly suppressed with TEA and 4-AP, while they were significantly suppressed with either SM or QND. These results suggest that mouse megakaryocytes possess K^+ conductance that was activated by extracellular alkalinization and that probably differs from conventional K^+ conductance in its pharmacological properties.

Keywords: Alkalinization-induced K^+ current, Mouse megakaryocyte, Voltage-gated K^+ current, K^+ channel blocker, pH-response

Megakaryocytes in bone marrow are the precursors from which blood platelets originate, and the regulation of megakaryocyte activity with their humoral stimulating factors such as thrombopoietin (1, 2) may lead to thrombocytopoiesis. Although the physiological significance of electrical activity of megakaryocytes remains to be determined, a variety of ionic channels are known to exist in the megakaryocyte membrane of various animal species including the following: voltage-gated delayed rectifier K^+ channels, voltage-gated Ca^{2+} channels and ADP-dependent Ca^{2+} -activated K^+ channels of the guinea pig megakaryocyte (3, 4) and type A voltage-gated K^+ channels, delayed rectifier K^+ channels and ATP-dependent Ca^{2+} -activated K^+ channels of the rat megakaryocyte (5–7). By coordinating the intracellular ionic composition, the membrane conductance with those ionic channels might contribute to making up proper conditions for the megakaryocyte functions, which presumably lead to megakaryocytopoiesis. In preliminary experiments with mouse megakaryocytes, we found that rapid alkaliniza-

tion but not acidification of the extracellular pH to >8.0 from the normal extracellular pH of 7.4 elicited outward current under voltage-clamped conditions. This alkaline-dependent membrane conductance might lead to the modulation of the excitability of mouse megakaryocytes under alkalosis conditions. As to pH-sensitive conductance in other tissues, acidification-induced responses have been well documented as proton-induced Na^+ currents of both peripheral (8–10) and central neurons (11). However, little is known about the alkalinization-induced current (I_{ALK}) with respect to its origin, physiological and pharmacological properties. Here, we report the electrophysiological and pharmacological properties of I_{ALK} in the mouse megakaryocyte and discuss its origin and physiological significance.

MATERIALS AND METHODS

Animals and cell dissociation

Adult BALB/c mice aged from 6 to 9 weeks were decapitated under ether anesthesia. The bone marrow cells were collected by gently flashing the bone marrow of

* To whom correspondence should be addressed.

the femoral bone of the animal with the normal external solution and dispersed by pipetting. After removing large pieces of tissue, the solution containing bone marrow cells was transferred to the 35-mm plastic dishes (Meridian, Okemos, MI, USA) containing a poly-L-lysine-coated cover-slip in the center of each dish. Megakaryocytes were identified on the basis of their size and morphology as described in the literature with guinea pig (3), rat (7) and mouse megakaryocytes (12, 13). Megakaryocytes isolated from adult mice had almost spherical shape with a diameter of 20 to 40 μm and exhibited a bright cell surface under phase-contrast microscopic observations.

Experimental solutions and drug application

The composition of the normal external solution was as follows: 150 mM NaCl, 5 mM KCl, 2 mM CaCl_2 , 1 mM MgCl_2 , 10 mM glucose and 10 mM HEPES (2-[4-(2-hydroxyethyl)-1-piperazinyl] ethanesulfonic acid) (pH 7.4). The low (pH 5.0–6.0) and high pH (pH 8.0–10.0) external solutions, respectively, contained PIPES (Piperazine-*N,N*-bis (2-ethanesulfonic acid)) and TAPS (*N*-Tris (hydroxymethyl) methyl-3-aminopropanesulfonic acid) instead of HEPES. The pH of these external solutions was adjusted with NaOH (1 N). A Na^+ - and Ca^{2+} -free external solution pH-adjusted with HCl (1 N) was prepared by substitution of Na^+ and Ca^{2+} of the normal external solution with *N*-methyl-D-glucamine cation (150 mM) and Mg^{2+} (5 mM), respectively. The composition of the pipette solution for the conventional patch-clamp technique that was used in most electrophysiological experiments in this study, was as follows: 150 mM KCl, 2 mM MgCl_2 , 10 mM EGTA (ethylenedis (oxonitrilo) tetra acetate) and 10 mM HEPES, while the pipette solution for the nystatin-perforated patch-clamp technique (14), which allowed the recording of caffeine-induced response, contained 150 mM KCl, 10 mM HEPES and nystatin to 200 $\mu\text{g}/\text{ml}$ as the final concentration. The pH of those pipette solutions was adjusted to 7.2 with KOH (1 N). Rapid change in the extracellular pH and application of drug-containing solutions were performed with a multi-barreled pipette technique (15).

Measurement of the membrane current

The conventional patch-clamp technique (16) was employed for the measurement of I_{ALK} , while the nystatin-perforated patch-clamp technique was applied for the recording of caffeine-induced Ca^{2+} -dependent currents. Patch-pipettes filled with the pipette solutions which showed an access resistance of 2–3 M Ω in the normal external solution, were used. By use of these recording pipettes, series resistance typically ranged from 5 to 8 M Ω and was compensated. Membrane currents were recorded under voltage-clamped conditions with a patch clamp

amplifier (CWZ-2300; Nihon Kohden, Tokyo), filtered at 3 KHz and simultaneously monitored on a storage oscilloscope (MS-5100A; Iwatsu, Tokyo) and a pen recorder (3057-11; Nishinohon-keisokuki, Tokyo), and stored on a digital audio tape recorder with custom designed modification (DTC-57ES; Sony, Tokyo) for further analysis. Recordings were carried out at room temperature (22–25°C).

Ratiometric measurement of $[\text{Ca}^{2+}]_i$

For measurements of $[\text{Ca}^{2+}]_i$, microscopic fura-2 ratio-metry was performed with the ARGUS50/CA system (Hamamatsu Photonix, Tokyo). Briefly, single mouse megakaryocytes fixed on a poly-L-lysine-coated glass coverslip in the center of 35-mm plastic dishes (Meridian) were incubated in the normal external solution containing 5 μM acetoxymethyl ester of fura-2 (fura-2/AM) for 20 min at 30°C in a dark room. After being loaded with fura-2/AM, mouse megakaryocytes were rinsed with normal external solution to remove the residual dye outside the cell completely and were then equilibrated for 30 min at room temperature. The fura-2-loaded mouse megakaryocytes were illuminated by alternately exciting them at 340 and 380 nm with a xenon lamp. The ratio of the fluorescence intensity at 340-nm excitation to that at 380-nm excitation was monitored and computer processed (U4469, Hamamatsu Photonix) to evaluate the change in $[\text{Ca}^{2+}]_i$. All experiments were performed at room temperature (22–25°C).

Statistics

Experimental data are given as the mean value \pm standard error of the mean (S.E.M.). Student's *t*-test was used to assess the significance of differences. *P* values of less than 0.05 were considered to be statistically significant.

Materials

Drugs and reagents employed in this study, namely HEPES, PIPES, TAPS, fura-2/AM and EGTA (Dojindo, Kumamoto); tetraethylammonium (Wako, Osaka), nystatin (Nacalai Tesque Kyoto); and 4-aminopyridine, streptomycin, quinidine and caffeine (Sigma, St. Louis, MO, USA) were purchased from suppliers as indicated.

RESULTS

I_{ALK}

Under voltage-clamped conditions, mouse megakaryocytes responded to extracellular alkalinization to pH >8.0 but not to acidification to pH <6.0, generating outward currents. Figure 1a shows a representative exam-

ple of I_{ALK} evoked at holding voltage (V_H) of -40 mV by application of the external solution pH-adjusted to 9.0. Downward deflections of the current in Fig. 1a, which were generated by repeated (at 0.2 Hz) hyperpolarization to -60 mV for 500 msec from the V_H , show conductance change during the generation of I_{ALK} . As shown in Fig. 1a, I_{ALK} was accompanied by an increase in the membrane conductance. Figure 1b shows I_{ALK} evoked at various extracellular pHs. I_{ALK} increased in amplitude when the extracellular pH was raised. The amplitude of I_{ALK} at each extracellular pH was normalized to that of I_{ALK} at the pH of 8.0 and was plotted against extracellular pH or concentrations of hydroxyl anion ($[OH^-]_o$) to make the

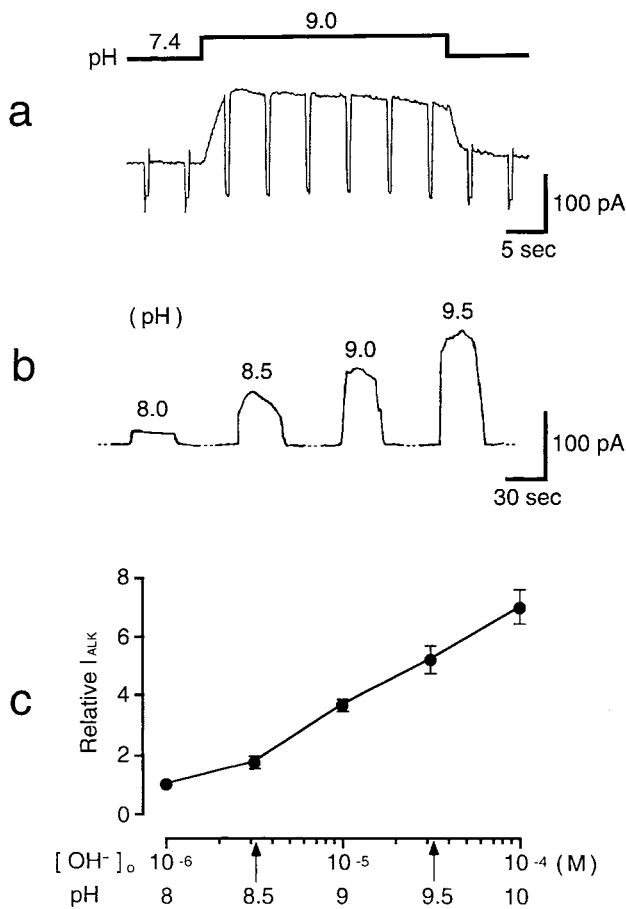


Fig. 1. Alkalinization-induced current (I_{ALK}) of mouse megakaryocytes. a: I_{ALK} evoked by extracellular alkalinization to pH of 9.0 from the normal pH of 7.4 at a holding voltage (V_H) of -40 mV. Downward deflection shows current evoked by repetitive hyperpolarization to -60 mV for 500 msec at 0.2 Hz. b: I_{ALK} evoked by application of external solutions of various pHs at V_H of -40 mV. The horizontal broken line indicates zero current level. c: Extracellular pH (dose)-response relationship of I_{ALK} . Abscissa: $[OH^-]_o$ or pH of the external solution applied, ordinate: relative amplitude of I_{ALK} when normalized to that of I_{ALK} evoked at extracellular pH of 8.0. Symbols and error bars indicate the mean \pm S.E.M. ($n=5$). All data were statistically significant at $P<0.05$.

extracellular pH-response relationship for I_{ALK} (Fig. 1c). Such an extracellular pH-response relationship of the generation of I_{ALK} was observed at pH values up to 10.0 ($n=5$), while at an extracellular pH over 11, I_{ALK} faded, and measurement of the current was difficult because of damage to the cell at such high pH. Therefore, it was not possible to obtain the maximal I_{ALK} at the extracellular pH range tested. Kinetics of activation and inactivation of I_{ALK} varied from cell to cell.

Voltage-dependence of I_{ALK}

In order to deduce the physiological significance of an ionic current, its voltage-dependence and identification of the carrier ions are important information. Figure 2a shows I_{ALK} evoked by the extracellular alkalinization to pH 8.5 at various V_H . The zero current is indicated by broken lines. I_{ALK} increased in amplitude when V_H was clamped to less negative voltage. Figure 2b shows the current-voltage (I-V) relationship for I_{ALK} when the amplitude of I_{ALK} at each V_H was normalized to that of I_{ALK} at -40 mV and plotted against V_H . The reversal potential for I_{ALK} , which was estimated by the extrapola-

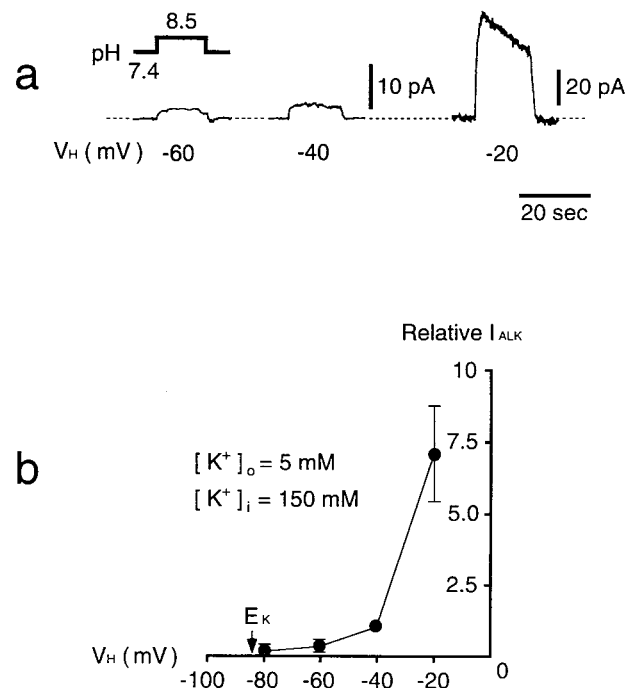


Fig. 2. Current-voltage (I-V) relationship of I_{ALK} . a: I_{ALK} evoked at various V_H values by application of the external solution pH-adjusted to 8.5. The horizontal broken line shows zero current level. b: I-V relationship of I_{ALK} . Abscissa: V_H , ordinate: relative amplitude of I_{ALK} when normalized to that of I_{ALK} at V_H of -40 mV. E_K is the equilibrium potential for K^+ , which was calculated with the Nernst equation, with $[K^+]_o$ and $[K^+]_i$ being 5 and 150 mM, respectively. Symbols and error bars indicate the mean \pm S.E.M. ($n=5$). All data were statistically significant at $P<0.05$.

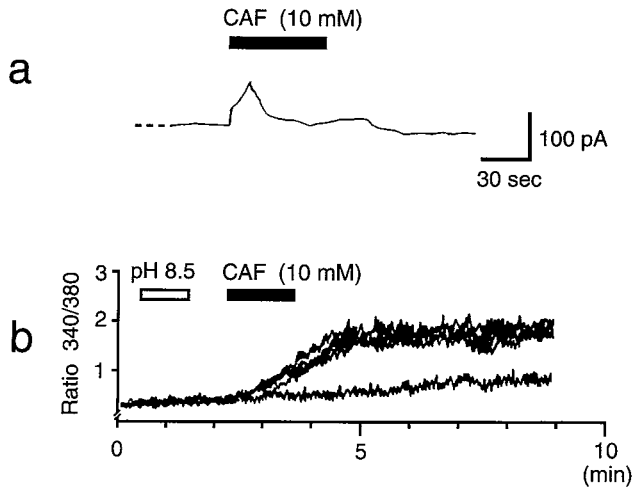


Fig. 3. Ca^{2+} -dependent responses of mouse megakaryocytes. **a:** Caffeine (CAF)-induced outward current of mouse megakaryocytes voltage-clamped at -20 mV with the nystatin-perforated patch-clamp technique. **b:** Effects of alkalization and caffeine on $[\text{Ca}^{2+}]_i$ that was measured with the fura 2 ratiometry. Open and closed bars indicate application of external solution pH-adjusted to 8.5 and caffeine, respectively.

tion of the I-V curve, was close to equilibrium potential for K^+ (E_K : -85 mV) that was calculated by use of the Nernst equation with $[\text{K}^+]_o$ and $[\text{K}^+]_i$ being 5 mM and 150 mM, respectively ($n=5$). This indicates that I_{ALK} was a K^+ current.

Ca^{2+} -dependent responses of mouse megakaryocytes

Figure 3a shows a representative example of caffeine-induced outward current of mouse megakaryocytes voltage-clamped at -20 mV with the nystatin-perforated patch-clamp technique. This caffeine-induced current was generated in all megakaryocytes tested ($n=5$) under this condition and was estimated to be a Ca^{2+} -activated K^+ current based on its reversal potential and dependency to extracellular Ca^{2+} (not shown). When caffeine was applied to the cells voltage-clamped with the conventional patch-pipettes filled with the EGTA (10 mM)-containing pipette solution that was employed for the recording of I_{ALK} in this study, caffeine-induced current was prevented in all megakaryocytes tested ($n=6$, not shown). I_{ALK} did not seem to be a Ca^{2+} -dependent current since I_{ALK} could

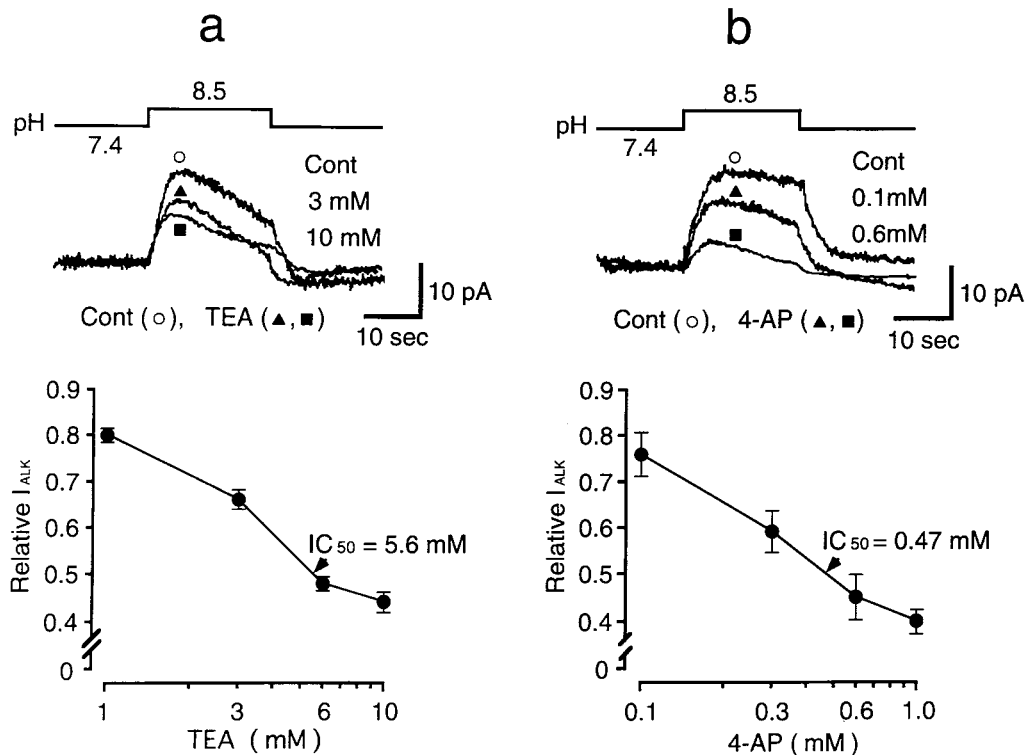


Fig. 4. Effects of tetraethylammonium (TEA) and 4-aminopyridine (4-AP) on I_{ALK} . **a** (upper panel): Effects of 3 (closed triangle) and 10 mM (closed square) TEA on I_{ALK} evoked by extracellular alkalization to pH of 8.5 in megakaryocytes voltage-clamped at -40 mV. **a** (lower panel): Concentration-effect relationship of TEA suppression of I_{ALK} . **b** (upper panel): Effects of 0.1 (closed triangle) and 0.6 mM (closed square) 4-AP on I_{ALK} . **b** (lower panel): Concentration-effect relationship of 4-AP suppression of I_{ALK} . Abscissa: concentration of K^+ channel blockers, ordinate: relative amplitude of I_{ALK} . IC_{50} : K^+ channel blockers concentrations at which the half maximal suppression of I_{ALK} occurred. Symbols and error bars indicate the mean \pm S.E.M. ($n=7$ for TEA and $n=5$ for 4-AP). All data were statistically significant at $P<0.05$.

be generated under such Ca^{2+} -buffered conditions with the conventional patch-pipettes. Moreover, the extracellular alkalinization to pH 8.5 produced no change in $[\text{Ca}^{2+}]_i$ in all megakaryocytes tested ($n=14$) when measured with the fura 2 ratiometry of $[\text{Ca}^{2+}]_i$ as shown in Fig. 3b.

Effects of K^+ channel blockers on I_{ALK}

As the reversal potential of I_{ALK} has indicated that I_{ALK} was a K^+ current, we examined the effects of several K^+ channel blockers on I_{ALK} and tried to characterize it pharmacologically. Figure 4a (upper panel) shows the effects of tetraethylammonium (TEA) on I_{ALK} evoked by extracellular alkalinization to pH 8.5. TEA was applied preliminarily 30 sec before the generation of I_{ALK} and subsequently I_{ALK} was evoked in presence of TEA at the indicated concentrations. TEA suppressed I_{ALK} in a concentration-dependent manner. To make the concentration-effect relationship of the TEA action on I_{ALK} , the amplitude of I_{ALK} in presence of TEA was normalized to that of the control I_{ALK} and the relative value of I_{ALK} was plotted against concentrations of TEA as shown in Fig. 4a (lower panel). The concentration of TEA required for the 50% suppression of I_{ALK} (IC_{50}) was 5.6 mM ($n=7$). Similarly, the effects of 4-aminopyridine (4-AP) were examined. Figure 4b (upper panel) shows the effects of

4-AP on I_{ALK} . 4-AP was applied with the same protocol that was used for TEA. 4-AP also suppressed I_{ALK} in a concentration-dependent manner ($n=5$) as shown in Fig. 4b (lower panel). The value of IC_{50} for 4-AP was 0.47 mM. Aminoglycoside antibiotics are known to suppress K^+ channels of cochlea hair cell (17, 18) and sarcoplasmic reticulum K^+ channels (19). In preliminary experiments, we found that streptomycin (SM) was a comparatively strong blocker of I_{ALK} . Figure 5a (left panel) shows the effects of SM on I_{ALK} . SM suppressed I_{ALK} in a concentration-dependent manner, similar to the effect of TEA or 4-AP. The concentration-effect relationship ($n=6$) of the SM action gave the IC_{50} value of 1.5 mM (Fig. 5b). Among the K^+ channel blockers, quinidine (QND) is known to block most types of K^+ channels except for inward rectifier and type A channels (20). In guinea pig megakaryocytes, Kawa has found that voltage-gated delayed rectifier K^+ current was significantly suppressed by quinine, a stereoisomer of QND (3). We then tested the effects of QND on I_{ALK} . In contrast to its great sensitivity to TEA, 4-AP and SM, I_{ALK} was completely resistant to QND in all megakaryocytes tested ($n=5$) when tested at concentrations up to nearly its maximal solubility in water (Fig. 5a, right panel and Table 1). These results suggest that the origin of the K^+ -conductance that generated I_{ALK} was pharmacologically distinct

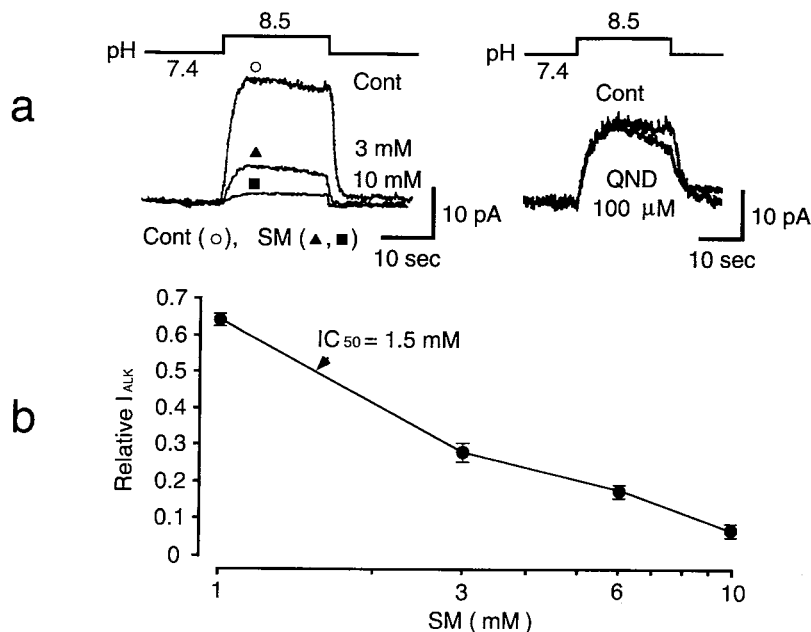


Fig. 5. Effects of streptomycin (SM) and quinidine (QND) on I_{ALK} . a (left panel): Effects of 3 (closed triangle) and 10 mM (closed square) SM on I_{ALK} evoked by extracellular alkalinization to pH of 8.5 in megakaryocytes voltage-clamped at -40 mV. a (right panel): Effects of 100 μM QND on I_{ALK} . b: Concentration-effect relationship of SM effects on I_{ALK} . Abscissa: concentration of SM, ordinate: relative amplitude of suppressed I_{ALK} , which was normalized to that of the control. IC_{50} : SM concentration at which the half maximal suppression of I_{ALK} occurred. Symbols and error bars indicate the mean \pm S.E.M. ($n=6$). All data were statistically significant at $P < 0.05$.

Table 1. Effects of K^+ channel blockers on I_{ALK} and I_K

	TEA	4-AP	SM	QND
I_{ALK}	$47.9 \pm 1.5^{**}$ (6 mM)	$45.2 \pm 4.9^{**}$ (0.6 mM)	$64.0 \pm 1.3^{**}$ (1 mM)	$98.0 \pm 2.0^{n.s.}$ (100 μ M)
I_K	$91.1 \pm 2.2^*$ (6 mM)	$92.9 \pm 0.8^{**}$ (0.6 mM)	$66.1 \pm 5.2^{**}$ (1 mM)	$75.6 \pm 3.4^{**}$ (100 μ M)

Relative amplitude of I_{ALK} or I_K in presence of each K^+ channel blocker is given as the mean $\% \pm$ S.E.M. ($n=7$ for I_{ALK} with TEA, $n=6$ for I_{ALK} with SM or $n=5$ for others) of the control I_{ALK} or I_K . Each K^+ channel blocker was applied at the concentration indicated in brackets. $n.s.$: non significant, $*P < 0.01$, $**P < 0.005$.

from conventional K^+ channels, including voltage-gated K^+ channels.

I_K of mouse megakaryocytes

Since the pharmacological characterization of I_{ALK} with those above K^+ channel blockers has suggested that I_{ALK} was distinct from the conventional I_K , we examined the effects of the same series of K^+ channel blockers, including TEA, 4-AP, SM and QND on I_K of the mouse megakaryocytes and compared the effects with those on I_{ALK} . Figure 6, a (closed circle) and b, shows representative examples of voltage-gated outward currents evoked by step depolarization to indicated stimulation voltages from V_H of -80 mV and its I-V relationship that was made by plotting the amplitude of the current against stimulation voltages. The reversal potential for the outward current was close to E_K , as shown in Fig. 6b, indicating that the current was a pure I_K . This was reproduced in all megakaryocytes tested ($n=6$). Figure 6a (open circle) shows the effects of TEA (6 mM), 4-AP (0.6 mM), SM (1.0 mM) and QND (100 μ M) on I_K . The concentration of each drug was chosen for the comparison of its effects on I_K with that on I_{ALK} (see Table 1). In contrast to their effects on I_{ALK} , TEA and 4-AP revealed weak suppression of I_K , while QND significantly suppressed I_K . SM was a nearly equipotent blocker for I_K and I_{ALK} . It is notable that I_{ALK} was completely resistant to QND that was a relatively strong blocker for I_K . As summarized in Table 1, I_{ALK} was pharmacologically distinct from I_K . Since a voltage-dependent inward current was rarely detected under the conditions of our experiments, the I-V relation for I_K and the effects of those K^+ channel blockers on I_K were not affected when the normal external solution was substituted by the Na^+ - and Ca^{2+} -free external solution (not shown).

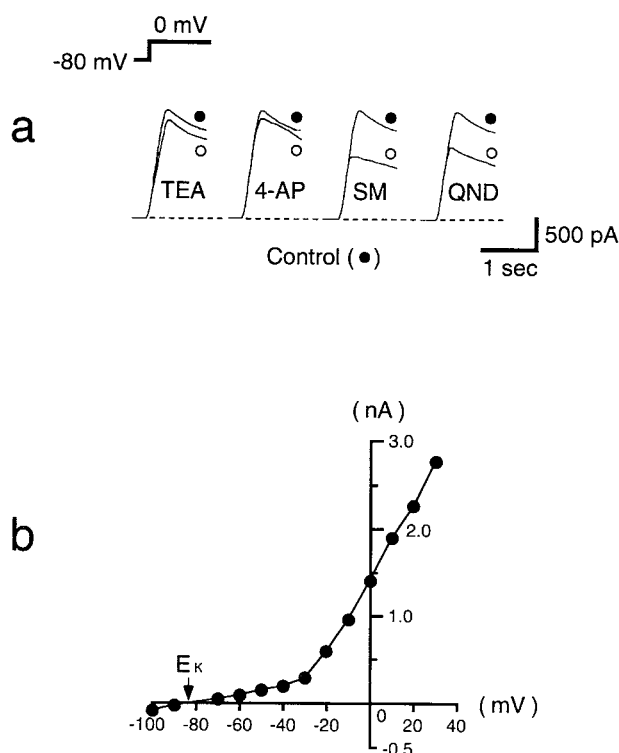


Fig. 6. Voltage-gated K^+ current (I_K) of mouse megakaryocytes and effects of K^+ channel blockers. a: Effects of K^+ channel blockers, including tetraethylammonium (TEA), 4-aminopyridine (4-AP), streptomycin (SM) and quinidine (QND) on I_K evoked by step depolarization to 0 mV from V_H of -80 mV. Closed and open circles indicate the control and suppressed I_K with K^+ channel blockers. b: Current-voltage relationship of I_K . Abscissa: stimulation voltage, ordinate: peak amplitude of I_K .

DISCUSSION

As pH-dependent membrane conductance, proton-induced cationic currents have been well documented (8–11). The mechanism underlying the generation of proton-induced currents has been elucidated by a transient transformation of voltage-gated Na^+ channels (11) and Ca^{2+} channels (8) from a voltage-gated state to a proton-gated state. A recent study that analyzed complementary DNA encoding proton-gated channels has demonstrated that a part of proton-gated channels belongs to the family of amiloride-sensitive cationic channels (21).

Little was known about alkalization-gated conductance before the finding of I_{ALK} in this study. I_{ALK} was proved to be a K^+ current based on its reversal potential close to E_K . Kinetics of I_{ALK} in its activation and inactivation varied from cell to cell. This variation made it difficult to determine whether the I_{ALK} kinetics is voltage- and/or pH-dependent. Whether I_{ALK} was generated by conventional K^+ channels by a transient transformation is an important question that asks about the origin of

I_{ALK} channel. I_{ALK} was efficiently suppressed by K^+ -channel blockers, including TEA and 4-AP, but was completely resistant to QND. SM, an aminoglycoside antibiotic whose analogue is known to suppress K^+ channels of cochlea hair cell (17, 18) and sarcoplasmic reticulum K^+ channels (19), also revealed comparatively strong suppression of I_{ALK} . Various types of ionic channels, including K^+ channels have been found in the megakaryocyte preparation of several animal species. Kawa (3, 4) has reported that guinea pig megakaryocytes have ADP-dependent K^+ channels and delayed rectifier K^+ channels besides voltage-sensitive Ca^{2+} channels. Type A voltage-gated K^+ channels have been recently found in rat megakaryocytes, although the authors have detected almost no voltage-dependent inward current (5). Similar to the rat megakaryocytes (5), voltage-gated inward current was rarely detected in the mouse megakaryocytes under the conditions of our experiments. We observed that voltage-gated K^+ currents of the mouse megakaryocyte were highly sensitive to QND and SM, but were only slightly suppressed by TEA and 4-AP. This indicates that the voltage-gated K^+ currents of mouse megakaryocytes were similar to the conventional voltage-gated K^+ currents in their drug sensitivity (20). In contrast, I_{ALK} was completely resistant to QND but highly sensitive to TEA, 4-AP and SM as shown in Figs. 4 and 5 and Table 1. These results suggest that I_{ALK} is generated by K^+ conductance that is distinct from the voltage-gated K^+ channels of the mouse megakaryocyte.

On the basis of its QND-resistance, I_{ALK} also seemed to be distinct from the K^+ currents of other tissues, including delayed rectifier K^+ currents, large conductance (BK) type Ca^{2+} -activated K^+ currents and ATP-dependent K^+ currents (20). ATP-induced oscillation of Ca^{2+} -activated K^+ current of rat megakaryocytes, which was resulted from the activation of purinoceptors, has been shown to involve inositol 1,4,5-trisphosphate-induced Ca^{2+} release as the underlying mechanism (6, 7). This ATP-induced oscillatory Ca^{2+} -activated K^+ current could be recorded by using the nystatin-perforated patch-clamp technique (6, 7). In the mouse megakaryocytes, the nystatin-perforated patch-clamp technique but not the conventional technique with the Ca^{2+} -buffered pipette solution allowed the generation of caffeine-induced Ca^{2+} -activated K^+ current (Fig. 3a). These results suggest that I_{ALK} was not Ca^{2+} -dependent since the Ca^{2+} -buffered pipette solution condition was strong enough to prevent the caffeine-induced Ca^{2+} -dependent current. Moreover, no change in $[Ca^{2+}]_i$ during the alkalinization protocol was observed when measured with the microscopic fura 2 ratiometry of $[Ca^{2+}]_i$ in contrast to the caffeine-induced response that produced significant $[Ca^{2+}]_i$ elevation in the same experiments.

It is concluded that mouse megakaryocytes possess K^+ conductance that was activated in response to extracellular alkalinization. I_{ALK} may contribute to modulation of electrical excitability of the megakaryocyte membrane under alkalosis conditions.

One can argue whether the pH range at which I_{ALK} was elicited can be achieved in the surroundings of megakaryocytes. Anatomically, bone marrow consists of a pattern of vessels and nerves, differentiated and undifferentiated hematopoietic cells, reticuloendothelial cells and fatty tissue, all of which are encased by the endosteum, which is a membrane lining the marrow cavity of the bone. Since the vascular system consists of a network of arterioles that empty into a complex system of venous sinusoids (22), the pH of the surroundings of megakaryocytes may be similar to that in the blood vessel. Local alkalosis that presumably depends upon the activity of stem cells involved in the marrow might occur and affect the extracellular pH of megakaryocytes.

Although the physiological significance of I_{ALK} is at present a matter for speculation, the alkalinization-induced response might contribute to the megakaryocyte functions, including thrombocytosis. It has been demonstrated that HL-60 promyelocytic leukemia cells differentiate in response to extracellular alkalinization to a pH (>7.6) similar to that required for generation of I_{ALK} and became eosinophiles, although the underlying mechanism has not yet been determined (23).

Further studies will be required to determine the roles of I_{ALK} in the megakaryocyte functions.

REFERENCES

- 1 Evatt BL and Levin J: Measurement of thrombopoiesis in rabbits using 75 selenomethionine. *J Clin Invest* **48**, 1615–1626 (1969)
- 2 Harker LA: Control of platelet production. *Annu Rev Med* **25**, 383–400 (1974)
- 3 Kawa K: Voltage-gated calcium and potassium currents in megakaryocytes dissociated from guinea-pig bone marrow. *J Physiol (Lond)* **431**, 187–206 (1990)
- 4 Kawa K: Guinea-pig megakaryocytes can respond to external ADP by activating Ca^{2+} -dependent potassium conductance. *J Physiol (Lond)* **431**, 207–224 (1990)
- 5 Elkin R and Sullivan R: Complexity of the outward K^+ current of the rat megakaryocyte. *Am J Physiol* **272**, C1525–C1531 (1997)
- 6 Uneyama H, Uneyama C and Akaike N: Intracellular mechanisms of cytoplasmic Ca^{2+} oscillation in rat megakaryocyte. *J Biol Chem* **268**, 168–174 (1993)
- 7 Uneyama C, Uneyama H and Akaike N: Cytoplasmic Ca^{2+} oscillation in rat megakaryocytes evoked by a novel type of purinoceptor. *J Physiol (Lond)* **470**, 731–749 (1993)
- 8 Davies NW, Lux HD and Morad M: Site and mechanism of activation of proton-induced sodium current in chick dorsal root ganglion neurones. *J Physiol (Lond)* **400**, 159–187 (1988)

- 9 Kovalchuk YN, Krishtal OA and Nowycky MC: The proton-activated inward current of rat sensory neurons includes a calcium component. *Neurosci Lett* **115**, 237–242 (1990)
- 10 Krishtal OA and Pidoplichko VI: A receptor for protons in the nerve cell membrane. *Neuroscience* **5**, 2325–2327 (1980)
- 11 Ueno S, Nakaye T and Akaike N: Proton-induced sodium current in freshly dissociated hypothalamic neurones of the rat. *J Physiol (Lond)* **447**, 309–327 (1992)
- 12 Cui Z, Reilly MP, Surrey S, Schwartz E and McKenzie SE: –245 bp of 5'-flanking region from the human platelet factor 4 gene is sufficient to drive megakaryocyte-specific expression in vivo. *Blood* **91**, 2326–2333 (1998)
- 13 Melford SK, Turner M, Briddon SJ, Tybulewicz VLJ and Watson SP: Syk and Fyn are required by mouse megakaryocytes for the rise in intracellular calcium induced by a collagen-related peptide. *J Biol Chem* **272**, 27539–27542 (1997)
- 14 Wakamori M, Hidaka H and Akaike N: Hyperpolarizing muscarinic responses of freshly dissociated rat hippocampal CA1 neurons. *J Physiol (Lond)* **463**, 585–604 (1993)
- 15 Carbone E and Lux HD: Kinetics and selectivity of a low-voltage-activated calcium current in chick and rat sensory neurones. *J Physiol (Lond)* **386**, 547–570 (1987)
- 16 Hamill OP, Marty A, Neher E, Sakmann B and Sigworth FJ: Improved patch-clamp techniques for high-resolution current recording from cells and cell-free membrane patches. *Pflügers Arch* **391**, 85–100 (1981)
- 17 Corey DP and Hudspeth AJ: Ionic basis of the receptor potential in a vertebrate hair cell. *Nature* **281**, 675–677 (1979)
- 18 Hudspeth AJ: Extracellular current flow and the site of transduction by vertebrate hair cells. *J Neurosci* **2**, 1–10 (1982)
- 19 Oosawa Y and Sokabe M: Voltage-dependent aminoglycoside blockade of the sarcoplasmic reticulum K^+ channel. *Am J Physiol* **250**, C361–C364 (1986)
- 20 Hille B: Potassium channels and chloride channels. In *Ionic Channels of Excitable Membrane*, Edited by Hill B, pp 130–133, Sinauer Associates, Inc, Sunderland, MA (1992)
- 21 Waldman R, Champigny G, Bassilana F, Heurteaux C and Lazdunski M: A proton-gated cation channel involved in acid-sensing. *Nature* **386**, 173–177 (1997)
- 22 Abboud CN and Lichtman MA: Structure of the marrow. In *Williams Hematology*, Edited by Beutler E, Lichtman MA, Coller BS and Kipps TJ, 5th edition, pp 25–38, McGraw-Hill, Inc, New York, NY (1995)
- 23 Fischkoff SA and Condon ME: Switch in differentiative response to maturation inducers of human promyelocytic leukemia cells by prior exposure to alkaline conditions. *Cancer Res* **45**, 2065–2069 (1985)